

Entanglement Rényi entropy and boson-fermion duality in massless Thirring model

Harunobu Fujimura, Tatsuma Nishioka and Soichiro Shimamori

*Department of Physics, Osaka University,
Machikaneyama-Cho 1-1, Toyonaka 560-0043, Japan*

ABSTRACT: We investigate the second Rényi entropy of two intervals in the massless Thirring model describing a self-interacting Dirac fermion in two dimensions. Boson-fermion duality relating this model to a free compact boson theory enables us to simplify the calculation of the second Rényi entropy, reducing it to the evaluation of the partition functions of the bosonic theory on a torus. We derive exact results on the second Rényi entropy, and examine the dependence on the sizes of the intervals and the coupling constant of the model both analytically and numerically. We also explore the mutual Rényi information, a measure quantifying the correlation between the two intervals, and find that it generally increases as the coupling constant of the Thirring model becomes larger.

Contents

1	Introduction	1
2	Boson-fermion duality	3
2.1	Fermionization on a torus	3
2.2	Compact boson/massless Thirring duality	5
3	Entanglement Rényi entropy in massless Thirring model	7
3.1	Replica method	7
3.2	Exact results on ERE and MRI	10
3.3	Parameter dependence of ERE and MRI	14
3.3.1	Cross-ratio dependence	14
3.3.2	Coupling dependence	16
3.4	EREs for other spin structures	17
4	Conclusion and Discussion	21
A	Formulas on theta function and Dedekind eta function	22
B	Detailed calculations of (2.25)	23

1 Introduction

Quantum entanglement, a fundamental phenomenon in modern physics characterized by non-local correlations between quantum states separated by distance, has garnered extensive attention not only in quantum information theory but also in high energy physics, condensed matter theory, and gravitation theory. In quantum field theory (QFT), various measures of quantum entanglement have proven to be indispensable tools for characterizing and classifying different phases of matter, particularly topological phases [1, 2], while also capturing universal scaling behaviors in critical systems [3–6]. Moreover, quantum entanglement has found an unexpected connection with gravitational physics via the holographic principle [7, 8], yielding fresh perspectives on the intricate structures of spacetime, including those governing black hole physics, as well as non-perturbative aspects of QFT. (See e.g., [9–13] for reviews.)

The entanglement Rényi entropy (ERE) is one of the principal measures that quantify the amount of quantum entanglement shared between different parts of a quantum system. They are a generalization of the more familiar measure known as entanglement entropy, defined by

$$S_n \equiv \frac{1}{1-n} \log \text{Tr}_V [\rho_V^n] , \quad (1.1)$$

where ρ_V is the reduced density matrix of a subsystem V and n is a parameter that can take on any positive real value. In QFT, the subsystem V is given by a subregion on a time slice, and the reduced density matrix ρ_V can be represented by the Euclidean path integral on a manifold with a cut along V . Hence, the calculation of the ERE amounts to that of the partition function Z_n on the replica manifold, which is an n -sheeted manifold branched over V . The codimension-two conical singularity around ∂V often prevents us from performing the path integral analytically on the replica manifold. The ERE has had exact results for general n only in simple cases to date, such as an interval in two-dimensional conformal field theories (CFTs) [3, 5], multiple intervals in free massless fermion theory [14], and spherical region in ($d \geq 3$)-dimensional free massless scalar and fermion theories [15]. Another exactly calculable case is the second ERE ($n = 2$) of two intervals in a two-dimensional free compact boson theory [16–18]. However, when it comes to incorporating interactions, the calculation of the ERE proves to be more challenging, and only a few approximate results have been obtained, such as in the $O(N)$ models in the large- N limit [19], so far.¹

In this paper, we calculate the ERE exactly in the massless Thirring model describing a self-interacting Dirac fermion in two dimensions [21];

$$\int d^2x \left[i \bar{\psi} \not{\partial} \psi + \frac{\pi}{2} \lambda (\bar{\psi} \gamma^\mu \psi) (\bar{\psi} \gamma_\mu \psi) \right]. \quad (1.2)$$

This model can be seen as a marginal deformation of a free massless Dirac fermion and enjoys conformal symmetry with central charge $c = 1$. Moreover, it possesses a duality with a free boson theory of a compact radius. We can leverage the boson-fermion duality to reduce the formidable calculation of the ERE in the interacting fermionic theory to a more manageable task in the free bosonic theory. Nevertheless, a subtlety arises when evaluating the ERE with the boson-fermion duality [22]. Since the replica manifold $\Sigma_{n,N}$ associated with the n -th ERE of N intervals is a Riemann surface of genus $g = (n-1)(N-1)$, fermionic theories depend on the spin structures along $2g$ one-cycles on $\Sigma_{n,N}$. On the other hand, the dual bosonic theories can be defined without specifying the spin structures, so their EREs do not appear to match unless $n = 1$ or $N = 1$. This apparent paradox is resolved by taking into account the coupling of the dual bosonic theory to a topological field theory (the Kitaev Majorana chain [23]), and the gauging of a non-anomalous \mathbb{Z}_2 symmetry [24–28]. We employ this refined perspective on the boson-fermion duality and derive the exact results on the second ERE of two intervals ($n = N = 2$) in the massless Thirring model.

This paper is structured as follows. In section 2, we provide a concise review of the modern formulation of boson-fermion duality for bosonic theories with a non-anomalous \mathbb{Z}_2 symmetry in two dimensions. While the duality extends to higher-genus Riemann surfaces, we concentrate on the torus case. We express the partition functions of fermionic theories with four distinct spin structures (periodic/anti-periodic boundary conditions along the two

¹By suitably extending the definition, the ERE admits an exact calculation in a certain class of interacting supersymmetric field theories [20].

one-cycles) in terms of the linear combinations of four bosonic partition functions which incorporate the background \mathbb{Z}_2 gauge fields. This sets the stage for the application of the Thirring/compact boson duality in the later sections. Section 3 begins with a brief account of the path integral formulation of the ERE in fermionic theories. We then proceed to derive exact results on the second ERE of two intervals as well as the mutual Rényi information, a measure quantifying the correlation between these intervals. We also examine their dependence on both interval sizes and the coupling constant analytically in some limits and numerically in broad parameter regions. Finally, section 4 is dedicated to discussion and potential directions for future works.

2 Boson-fermion duality

Boson-fermion duality makes it much easier for us to go back and forth between a bosonic theory and a fermionic one. In particular, we can construct a two-dimensional fermionic theory \mathcal{T}_F from a bosonic one \mathcal{T}_B via the fermionization dictionary [27, 28];

$$\mathcal{T}_F = \frac{\mathcal{T}_B \times \text{Kitaev}}{\mathbb{Z}_2^B}, \quad (2.1)$$

where \mathbb{Z}_2^B is a non-anomalous global symmetry in the bosonic theory. In this section, we firstly expand on the procedure incorporating the relation (2.1). We next rewrite the partition function of the massless Thirring model in terms of those of a free compact boson model by applying the fermionization dictionary (2.1).

2.1 Fermionization on a torus

Given a bosonic theory \mathcal{T}_B with a \mathbb{Z}_2 symmetry, the construction of a corresponding fermionic theory \mathcal{T}_F proceeds through the following two steps:

- Couple the bosonic theory \mathcal{T}_B with the spin topological QFT (TQFT) Kitaev.
- Gauge the diagonal \mathbb{Z}_2^B symmetry of the theory $\mathcal{T}_B \times \text{Kitaev}$.

The fermionization procedure is applicable on any Riemann surface, but for the sake of simplicity, we will focus our attention on the case of a torus \mathbf{T} below.

First of all, Kitaev is the fermionic spin TQFT associated with a given \mathbb{Z}_2^B global symmetry, defined by the partition function

$$\text{Kitaev} : (-1)^{\text{Arf}[T+\bar{\rho}]+\text{Arf}[\bar{\rho}]}, \quad (2.2)$$

where $T \in H^1(\mathbf{T}, \mathbb{Z}_2^B)$ is the background gauge field associated with \mathbb{Z}_2^B symmetry, and characterized by holonomy around the two one-cycles γ_1 and γ_2 of \mathbf{T} ;

$$T = (T_1, T_2), \quad T_I \equiv \int_{\gamma_I} T \in \{0, 1\}, \quad I = 1, 2. \quad (2.3)$$

Also, $\tilde{\rho}$ is the spin structure in the fermionic theory \mathcal{T}_F . On a torus, there are four choices of the spin structure depending on whether the fermionic field subjects to the periodic (P) or anti-periodic (A) boundary condition for each one-cycle on \mathbf{T} : $\tilde{\rho} = \text{PP}, \text{AP}, \text{PA}, \text{AA}$. In addition, $\text{Arf}[\tilde{\rho}]$ is the Arf invariant, which takes its value in zero or one depending on the spin structure $\tilde{\rho}$;

$$\text{Arf}[\tilde{\rho}] = \begin{cases} 0 & \tilde{\rho} = \text{AP}, \text{PA}, \text{AA}, \\ 1 & \tilde{\rho} = \text{PP}. \end{cases} \quad (2.4)$$

We should note that the insertion of a non-trivial background \mathbb{Z}_2^B gauge field T along a one-cycle γ changes the spin structure associated with γ . For instance, the holonomy of the \mathbb{Z}_2^B gauge field with its value $(1, 0)$ shifts the spin structures as follows:

$$\text{PP} \rightarrow \text{AP}, \quad \text{AP} \rightarrow \text{PP}, \quad \text{PA} \rightarrow \text{AA}, \quad \text{AA} \rightarrow \text{PA}, \quad (2.5)$$

and thereby the Arf invariant $\text{Arf}[(1, 0) + \tilde{\rho}]$ is given by

$$\text{Arf}[(1, 0) + \tilde{\rho}] = \begin{cases} 0 & \tilde{\rho} = \text{PP}, \text{AA}, \text{PA}, \\ 1 & \tilde{\rho} = \text{AP}. \end{cases} \quad (2.6)$$

Similar considerations apply straightforwardly to the other gauge configurations. At the level of the partition function, coupling the bosonic theory \mathcal{T}_B to the TQFT Kitaev amounts multiplying the bosonic torus partition function $Z_B[T]$ with the TQFT defined by (2.2);

$$\mathcal{T}_B \times \text{Kitaev} : Z_B[T] (-1)^{\text{Arf}[T+\tilde{\rho}]+\text{Arf}[\tilde{\rho}]} . \quad (2.7)$$

Next, we proceed to perform the gauging of the \mathbb{Z}_2^B global symmetry. This means that we promote the background gauge field T to the dynamical one t , and sum over all configurations of the gauge field t . This summation is a finite dimensional analog of the usual path integral, and the resulting gauged theory $(\mathcal{T}_B \times \text{Kitaev})/\mathbb{Z}_2^B$ can be written as follows:

$$\frac{\mathcal{T}_B \times \text{Kitaev}}{\mathbb{Z}_2^B} : \frac{1}{2} \sum_{t \in H^1(\mathbf{T}, \mathbb{Z}_2^B)} Z_B[t] (-1)^{\text{Arf}[t+\tilde{\rho}]+\text{Arf}[\tilde{\rho}]} . \quad (2.8)$$

The fermionization dictionary (2.1) asserts that (2.8) is exactly the same as the fermionic torus partition function,

$$Z_F[\tilde{\rho}] = \frac{1}{2} \sum_{t \in H^1(\mathbf{T}, \mathbb{Z}_2^B)} Z_B[t] (-1)^{\text{Arf}[t+\tilde{\rho}]+\text{Arf}[\tilde{\rho}]} . \quad (2.9)$$

By performing the summation in (2.9) with (2.4) and (2.6), we find

$$Z_F[\text{PP}] = \frac{1}{2} (Z_B[00] - Z_B[01] - Z_B[10] - Z_B[11]) , \quad (2.10)$$

$$Z_F[\text{AP}] = \frac{1}{2} (Z_B[00] + Z_B[01] - Z_B[10] + Z_B[11]) , \quad (2.11)$$

$$Z_F[\text{PA}] = \frac{1}{2} (Z_B[00] - Z_B[01] + Z_B[10] + Z_B[11]) , \quad (2.12)$$

$$Z_F[\text{AA}] = \frac{1}{2} (Z_B[00] + Z_B[01] + Z_B[10] - Z_B[11]) , \quad (2.13)$$

where we use a shorthand notation $Z_B[ab]$ for the partition function $Z_B[(a, b)]$.

2.2 Compact boson/massless Thirring duality

In this subsection, we apply the fermionization dictionary (2.9) to the massless Thirring model whose partition function $Z_F[\tilde{\rho}, \lambda, \tau]$ on a torus \mathbf{T} with a modulus τ is given by

$$Z_F[\tilde{\rho}, \lambda, \tau] \equiv \int \mathcal{D}\bar{\psi} \mathcal{D}\psi e^{-I[\tilde{\rho}, \lambda, \tau]} , \quad (2.14)$$

where $I[\tilde{\rho}, \lambda, \tau]$ is the massless Thirring action defined by [21]

$$I[\tilde{\rho}, \lambda, \tau] \equiv \int_{\mathbf{T}} d^2x \left[i \bar{\psi} \mathcal{D}_{\tilde{\rho}} \psi + \frac{\pi}{2} \lambda (\bar{\psi} \gamma^\mu \psi)(\bar{\psi} \gamma_\mu \psi) \right] . \quad (2.15)$$

Here, $\mathcal{D}_{\tilde{\rho}}$ is the Dirac operator with a spin structure $\tilde{\rho}$ and λ is the coupling constant, which will be referred to as the Thirring coupling in this paper.

The bosonic counterpart is a free compact boson theory whose torus partition function $Z_B[T, R, \tau]$ is defined by

$$Z_B[T, R, \tau] \equiv \int \mathcal{D}\phi \exp \left[-\frac{R^2}{8\pi} \int_{\mathbf{T}} d^2x (D_T \phi)^2 \right] , \quad (2.16)$$

where ϕ is the compact boson field with the periodicity 2π , and T is the \mathbb{Z}_2^{B} gauge field. Also, R is the compact radius, which is related to the Thirring coupling λ as follows [29]:

$$\frac{4}{R^2} = 1 + \lambda . \quad (2.17)$$

When the modulus is set to be pure-imaginary, $\tau = i\ell$, the torus partition function $Z_B[T, R, i\ell]$ is given by the following simple form:

$$Z_B[00, R, i\ell] = \frac{1}{\eta(i\ell)^2} \vartheta_3 \left(i \frac{2\ell}{R^2} \right) \vartheta_3 \left(i \frac{R^2 \ell}{2} \right) , \quad (2.18)$$

$$Z_B[01, R, i\ell] = \frac{1}{\eta(i\ell)^2} \vartheta_3 \left(i \frac{2\ell}{R^2} \right) \vartheta_2 \left(i \frac{R^2 \ell}{2} \right) , \quad (2.19)$$

$$Z_B[10, R, i\ell] = \frac{1}{\eta(i\ell)^2} \vartheta_4 \left(i \frac{2\ell}{R^2} \right) \vartheta_3 \left(i \frac{R^2 \ell}{2} \right) , \quad (2.20)$$

$$Z_B[11, R, i\ell] = \frac{1}{\eta(i\ell)^2} \vartheta_4 \left(i \frac{2\ell}{R^2} \right) \vartheta_2 \left(i \frac{R^2 \ell}{2} \right) , \quad (2.21)$$

where η is the Dedekind eta function [30]

$$\eta(\tau) = q^{\frac{1}{24}} \prod_{n=1}^{\infty} (1 - q^n), \quad q \equiv e^{2\pi i \tau}, \quad (2.22)$$

and ϑ_i ($i = 2, 3, 4$) are the Jacobi theta functions [30]

$$\vartheta_2(\tau) = \sum_{n \in \mathbb{Z} + \frac{1}{2}} q^{\frac{n^2}{2}}, \quad \vartheta_3(\tau) = \sum_{n \in \mathbb{Z}} q^{\frac{n^2}{2}}, \quad \vartheta_4(\tau) = \sum_{n \in \mathbb{Z}} (-1)^n q^{\frac{n^2}{2}}. \quad (2.23)$$

The fermionization dictionary (2.9) allows us to write the fermionic partition function $Z_F[\rho, \lambda, \tau]$ as the summation of the bosonic ones:

$$Z_F[\rho, \lambda, \tau] = \frac{1}{2} \sum_{t \in H^1(\mathbf{T}, \mathbb{Z}_2^{\mathbb{B}})} Z_B[t, R, \tau] (-1)^{\text{Arf}[t+\rho] + \text{Arf}[\rho]}. \quad (2.24)$$

Therefore, by plugging (2.18)-(2.21) into (2.24), we arrive at the exact formula for the torus partition function of the massless Thirring model (see appendix B for detail):

$$Z_F[\text{AA}, \lambda, i\ell] = \frac{1}{\sqrt{2} \eta(i\ell)^2} \left[\sum_{j=2}^4 \Xi_j(\lambda, i\ell) \right]^{\frac{1}{2}}, \quad (2.25)$$

$$Z_F[\text{AP}, \lambda, i\ell] = \frac{1}{\sqrt{2} \eta(i\ell)^2} \left[\sum_{j=2}^4 (1 - 2\delta_{j,2}) \Xi_j(\lambda, i\ell) \right]^{\frac{1}{2}}, \quad (2.26)$$

$$Z_F[\text{PA}, \lambda, i\ell] = \frac{1}{\sqrt{2} \eta(i\ell)^2} \left[\sum_{j=2}^4 (1 - 2\delta_{j,4}) \Xi_j(\lambda, i\ell) \right]^{\frac{1}{2}}, \quad (2.27)$$

$$Z_F[\text{PP}, \lambda, i\ell] = \frac{f(\lambda)}{\sqrt{2} \eta(i\ell)^2} \left[\sum_{j=2}^4 (2\delta_{j,3} - 1) \Xi_j(\lambda, i\ell) \right]^{\frac{1}{2}}, \quad (2.28)$$

where we define Ξ_j ($j = 2, 3, 4$) by

$$\Xi_j(\lambda, i\ell) \equiv \vartheta_j^2(i\ell(1+\lambda)) \vartheta_j^2\left(\frac{i\ell}{1+\lambda}\right), \quad (2.29)$$

and $f(\lambda)$ by

$$f(\lambda) \equiv \text{sgn} \left[\vartheta_2^2(i\ell(1+\lambda)) \vartheta_3^2\left(\frac{i\ell}{1+\lambda}\right) - \vartheta_3^2(i\ell(1+\lambda)) \vartheta_2^2\left(\frac{i\ell}{1+\lambda}\right) \right]. \quad (2.30)$$

Here, sgn is the sign function. We will employ these formulas (2.25)-(2.28) to calculate the ERE in the massless Thirring model in section 3.

Before closing this section, we make a comment on the action of the T-duality in the compact boson theory on the massless Thirring model. We should first note that the reflection

positivity restricts the coefficient of the kinetic term in the compact boson theory to be positive, and hence (2.17) leads to a valid range for the Thirring coupling: $\lambda > -1$. This is however not the end of the story, since there are equivalent points under the T-duality. Indeed, the T-duality in the compact boson theory maps the radius R to its inverse (see section 3.5 in the literature [27] for detail) as

$$\text{T-duality} \quad : \quad R \rightarrow R_{\text{dual}} \equiv \frac{4}{R}, \quad (2.31)$$

which acts as the T-duality transformation on the Thirring coupling via (2.17);

$$\text{T-duality} \quad : \quad \lambda \rightarrow \lambda_{\text{dual}} \equiv -\frac{\lambda}{\lambda + 1}. \quad (2.32)$$

It follows that the T-duality swaps the two coupling regions: $(-1, 0]$ and $[0, \infty)$, hence the fundamental domain of the Thirring coupling is either $(-1, 0]$ or $[0, \infty)$.

3 Entanglement Rényi entropy in massless Thirring model

We are now in position to derive the ERE and the mutual Rényi information (MRI) in the massless Thirring model. In section 3.1, we present a brief review on the replica method for calculating ERE in fermionic systems [10]. In section 3.2, we derive the ERE in the massless Thirring model by utilizing the boson-fermion duality introduced in section 2. In section 3.3 and 3.4, we examine the ERE and the MRI in the massless Thirring model by varying both the cross-ratio and the Thirring coupling.

3.1 Replica method

To introduce an ERE, we first divide the total space into V and \bar{V} . Here, V is the disjoint union of N intervals:

$$V \equiv [u_1, v_1] \cup [u_2, v_2] \cup \cdots \cup [u_N, v_N], \quad (3.1)$$

and \bar{V} is the complementary region to V . (See figure 1 for $N = 2$ case.) Throughout this paper, we assume that the state associated with the total space is vacuum $|0\rangle$, then the density matrix of the total space is $\rho_{\text{tot}} = |0\rangle\langle 0|$. The reduced density matrix of the region V is defined by tracing ρ_{tot} over all degree of freedom in \bar{V} ;

$$\rho_V \equiv \text{Tr}_{\bar{V}}[\rho_{\text{tot}}] = \text{Tr}_{\bar{V}}[|0\rangle\langle 0|]. \quad (3.2)$$

The n -th ERE $S_n(V)$ of the region V is defined by

$$S_n(V) \equiv \frac{1}{1-n} \log \text{Tr}_V[\rho_V^n], \quad n \in \mathbb{Z}_+. \quad (3.3)$$

We should note that, by analytically continuing a positive integer n to a real number and taking the limit $n \rightarrow 1$, ERE reduces to the entanglement entropy $S(V)$:

$$\lim_{n \rightarrow 1} S_n(V) = S(V) \equiv -\text{Tr}_V[\rho_V \log \rho_V]. \quad (3.4)$$

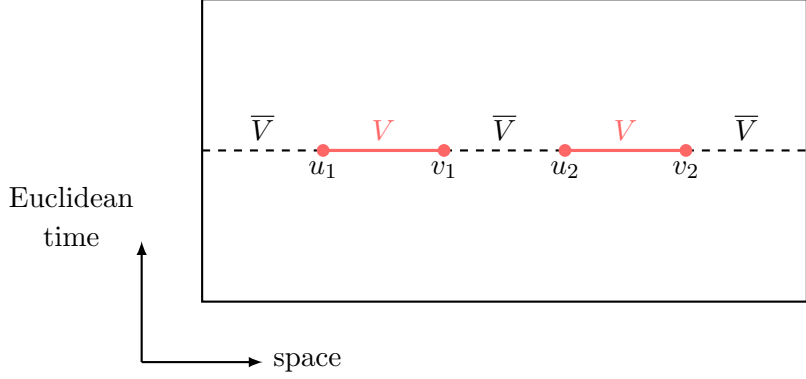


Figure 1. The regions V and \bar{V} in two dimensions for two intervals case. The entangling regions V is shown in red, whose end points are denoted by u_1, v_1, u_2 and v_2 .

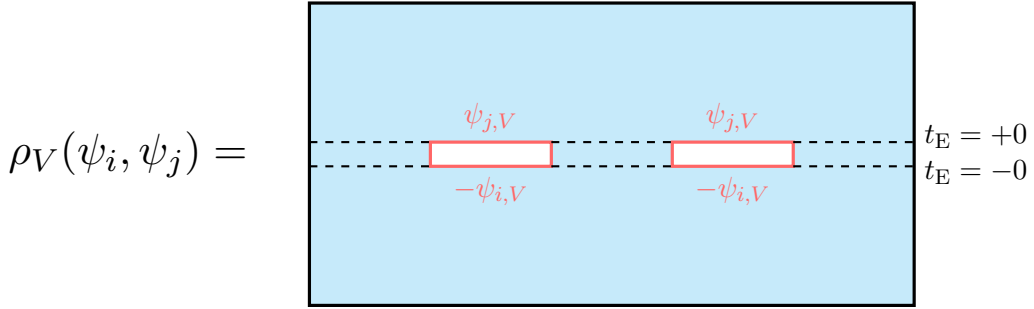


Figure 2. The path integral representation of the reduced density matrix. The cuts along the entangling regions V are shown in red. The path integral is performed over the blue region with the appropriate boundary conditions on V .

We can also introduce the n -th MRI $I_n(V_1, V_2)$ by

$$I_n(V_1, V_2) \equiv S_n(V_1) + S_n(V_2) - S_n(V_1 \cup V_2) , \quad (3.5)$$

where V_1 and V_2 are disjoint unions of the entangling region V such that $V = V_1 \cup V_2$. While ERE depends on the choice of the ultraviolet (UV) cutoff in QFT, MRI is known to be finite and independent of the regularization scheme [18]. Intuitively, MRI quantifies how the two regions V_1 and V_2 are entangled with each other.

In order to derive ERE and MRI, we use the replica method to evaluate $\text{Tr}_V \rho_V^n$. In the rest of this subsection, we describe the replica method by focusing on the fermionic theory. First of all, we rewrite the $\text{Tr}_V \rho_V^n$ in the following matrix multiplication form:

$$\text{Tr}_V [\rho_V^n] = \sum_{\psi_1, \psi_2, \dots, \psi_n} \rho_V(\psi_1, \psi_2) \rho_V(\psi_2, \psi_3) \cdots \rho_V(\psi_n, \psi_1) . \quad (3.6)$$

Here, $\rho_V(\psi_i, \psi_j)$ is the matrix element of the reduced density matrix ρ_V , defined by²

$$\begin{aligned} \rho_V(\psi_i, \psi_j) &\equiv \langle \psi_{i,V} | \rho_V | \psi_{j,V} \rangle \\ &= \frac{1}{Z_1} \int_{\psi(x \in V, t_E = -0) = -\psi_{i,V}}^{\psi(x \in V, t_E = +0) = \psi_{j,V}} \mathcal{D}\psi \mathcal{D}\bar{\psi} e^{-I[\psi, \bar{\psi}]} , \end{aligned} \quad (3.7)$$

where Z_1 is the partition function over the two-dimensional spacetime without entangling regions, and the minus sign appearing in the boundary condition stems from the fermionic statistics. We refer the reader to figure 2 for the illustration of the matrix element $\rho_V(\psi_i, \psi_j)$. From (3.6) and (3.7), $\text{Tr}_V [\rho_V^n]$ is given by the partition function $Z_{n,N}$ on the n -sheeted manifold $\Sigma_{n,N}$ which consists of n -copies of the original manifold with an appropriate gluing conditions along with the entangling region V :

$$\text{Tr}_V [\rho_V^n] = \frac{Z_{n,N}}{Z_1^n} \equiv \frac{1}{Z_1^n} \int_{\Sigma_{n,N}} \mathcal{D}\Psi \mathcal{D}\bar{\Psi} e^{-I[\Psi, \bar{\Psi}]} , \quad (3.8)$$

where Ψ denotes the n -vector of the fermionic fields defined by

$$\Psi \equiv (\psi_1, \psi_2, \dots, \psi_n)^T . \quad (3.9)$$

Furthermore, $\int_{\Sigma_{n,N}}$ means the restricted path integral with the following gluing conditions:

$$\Psi(x \in V, t_E = +0) = T \Psi(x \in V, t_E = -0) , \quad (3.10)$$

where T is the $n \times n$ matrix given by

$$T \equiv \begin{pmatrix} 0 & 1 & & & \\ & \ddots & \ddots & & \\ & & \ddots & \ddots & \\ & & & \ddots & 1 \\ (-1)^{n+1} & & & & 0 \end{pmatrix} . \quad (3.11)$$

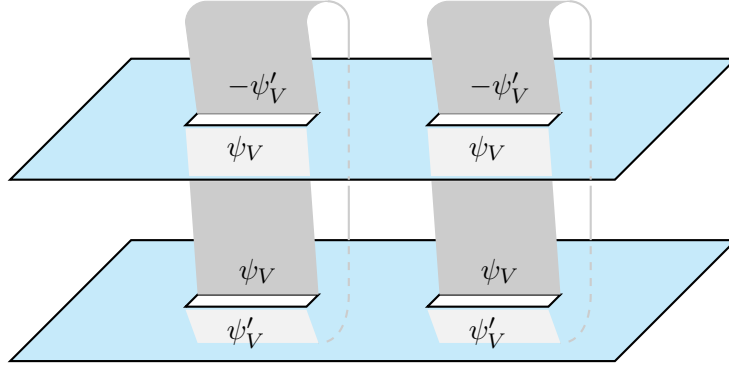
Figure 3 shows a graphical representation of (3.8) for the case of $(n, N) = (2, 2)$. By substituting (3.8) into the definition of the ERE (3.3), we can express the n -th ERE in terms of the partition function $Z_{n,N}$ on the n -sheeted manifold $\Sigma_{n,N}$:

$$S_n(V) = \frac{1}{1-n} \log \left[\frac{Z_{n,N}}{(Z_1)^n} \right] . \quad (3.12)$$

There are a few exact results of EREs derived by the replica method as listed below:

- Two-dimensional CFT:

²We normalize the overall factor of the state vector $|\psi_{i,V}\rangle$ so that $\text{Tr}_V \rho_V = 1$.



$$\Sigma_{2,2}$$

Figure 3. $\text{Tr}_V \rho_V^2$ can be written as the path integral over the two-sheeted manifold $\Sigma_{2,2}$ with the proper gluing conditions (3.10) up to some normalization factor.

In the case of one interval, the n -th ERE in an arbitrary CFT is given by [3]³

$$S_n^c([u, v]) = \frac{c}{6} \left(1 + \frac{1}{n}\right) \log \left(\frac{v-u}{\epsilon}\right). \quad (3.13)$$

where ϵ is UV cutoff length and c is the central charge in CFT. We emphasize that the coefficient in front of the logarithm depends only on the central charge and the number of sheets, hence is scheme-independent.

- Free massless Dirac fermion in two dimensions:

The n -th ERE of arbitrary N intervals in the free massless Dirac fermion is calculated in [14]. In particular, in the case $(n, N) = (2, 2)$, the ERE is given by

$$S_2^{\text{Free}}(V) = \frac{1}{4} \log \left(\frac{v_1 - u_1}{\epsilon} \cdot \frac{v_2 - u_2}{\epsilon}\right) + \frac{1}{4} \log(1-x), \quad (3.14)$$

where ϵ is the UV cutoff length and x is the cross-ratio defined by

$$x = \frac{(v_1 - u_1)(v_2 - u_2)}{(u_2 - u_1)(v_2 - v_1)}. \quad (3.15)$$

The exact results mentioned above (3.13) and (3.14) will be repeatedly used throughout the remainder of this paper.

3.2 Exact results on ERE and MRI

Now, we turn to the derivation of the ERE with $(n, N) = (2, 2)$ in the massless Thirring model (1.2) on the two-dimensional plane \mathbb{R}^2 . In general, it is challenging to calculate the

³Here we drop off the scheme dependent term.

Riemann surface	Spin structure	Periodicity condition			
$\Sigma_{2,2}$	ρ	PP	AP	PA	AA
\mathbf{T}	$\tilde{\rho}$	AA	PA	AP	PP

Table 1. Spin structures on the two-sheeted manifold $\Sigma_{2,2}$ (above) and the torus \mathbf{T} (below).

ERE in an interacting system, nevertheless, we can obtain the exact formula of the ERE in the massless Thirring model (1.2) by making full use of the boson-fermion duality described in section 2.

By applying the replica formula (3.12), the ERE with $(n, N) = (2, 2)$ is given by

$$S_2^\rho(V, \lambda) = -\log \left[\frac{Z_{2,2}(V, \lambda, \rho)}{(Z_1)^2} \right], \quad (3.16)$$

where Z_1 and $Z_{2,2}(V, \lambda, \rho)$ are the partition functions of the massless Thirring model on the two-dimensional plane \mathbb{R}^2 and the two-sheeted manifold $\Sigma_{2,2}$, respectively. Moreover, ρ denotes the spin structure on $\Sigma_{2,2}$. Since $\Sigma_{2,2}$ can be mapped to the torus \mathbf{T} by using the conformal transformation, the partition function can be written as [31]

$$\frac{Z_{2,2}(V, \lambda; \rho)}{(Z_1)^2} = \left(\frac{v_1 - u_1}{\epsilon} \cdot \frac{v_2 - u_2}{\epsilon} \right)^{-\frac{1}{4}} x^{\frac{1}{4}} (2^8 x(1-x))^{-\frac{1}{12}} Z_F[\tilde{\rho}, \lambda, i\ell], \quad (3.17)$$

where ϵ is the UV cutoff length and $Z_F[\tilde{\rho}, \lambda, i\ell]$ is the torus partition function of the massless Thirring with the complex structure modulus $\tau = i\ell$ defined in (2.14). Also, x is the cross-ratio defined by (3.15) and it can be also written in terms of the modulus $i\ell$:

$$x = \left(\frac{\vartheta_2(i\ell)}{\vartheta_3(i\ell)} \right)^4, \quad 1-x = \left(\frac{\vartheta_4(i\ell)}{\vartheta_3(i\ell)} \right)^4, \quad (3.18)$$

where $\vartheta_j(\tau)$ ($j = 2, 3, 4$) are Jacobi theta functions (2.23). Furthermore, $\tilde{\rho}$ is the spin structure on the torus \mathbf{T} . Note that the periodicity of the fermionic field changes under the conformal map from $\Sigma_{2,2}$ to \mathbf{T} . The relation between the spin structures ρ and $\tilde{\rho}$ is shown in table 1 (see also figure 4). By substituting (3.17) into (3.16), we can rewrite the ERE with $(n, N) = (2, 2)$ in the massless Thirring model as

$$S_2^\rho(V, \lambda) = \frac{1}{4} \log \left(\frac{v_1 - u_1}{\epsilon} \cdot \frac{v_2 - u_2}{\epsilon} \right) + \frac{1}{12} \log (2^8 x^{-2}(1-x)) - \log Z_F[\tilde{\rho}, \lambda, i\ell]. \quad (3.19)$$

In what follows, we focus on the case where the spin structure on $\Sigma_{2,2}$ is periodic for both one-cycles $\rho = \text{PP}$. This choice of the spin structure is quite natural from the view point of the gluing condition (3.10) (see also figure 3 and figure 4). We relegate the analysis on the ERE for the other spin structures to section 3.4.

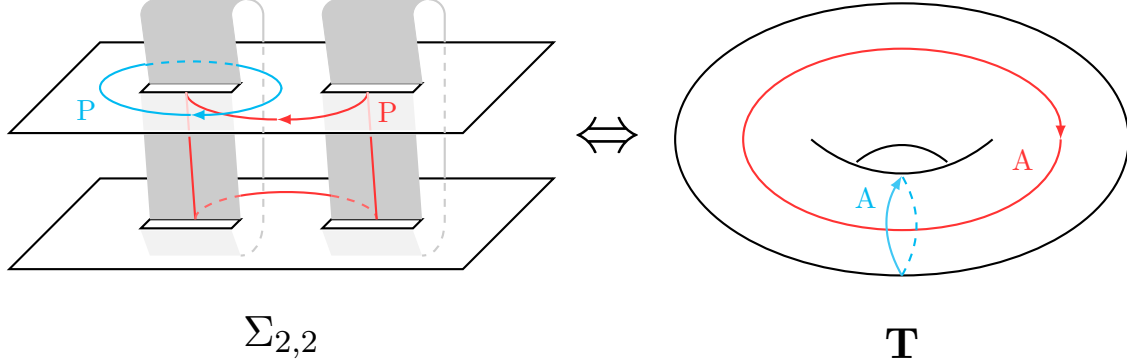


Figure 4. Two-sheeted manifold $\Sigma_{2,2}$ is conformally equivalent to the torus. By using the conformal map, the two cycles (red and blue lines) on $\Sigma_{2,2}$ are mapped to the corresponding cycles on the torus as depicted in the above figure. Note that the periodic boundary conditions on $\Sigma_{2,2}$ are changed to the anti-periodic ones on the torus.

By substituting the boson-fermion duality (2.25) to (3.19), we obtain the exact formula of the ERE in the massless Thirring model with the spin structure $\rho = \text{PP}$:

$$S_2^{\text{PP}}(V, \lambda) = S_2^{\text{PP}}(V, 0) - \frac{1}{2} \log \left[\frac{1}{2\vartheta_3^4(i\ell)} \sum_{j=2}^4 \Xi_j(\lambda, i\ell) \right], \quad (3.20)$$

where $S_2^{\text{PP}}(V, 0)$ is given by

$$S_2^{\text{PP}}(V, 0) = \frac{1}{4} \log \left(\frac{v_1 - u_1}{\epsilon} \cdot \frac{v_2 - u_2}{\epsilon} \right) + \frac{1}{4} \log(1 - x). \quad (3.21)$$

We should note that $S_2^{\text{PP}}(V, 0)$ obtained via the boson-fermion duality is consistent with the known result $S_2^{\text{Free}}(V)$ in (3.14). For later convenience, we define the deviation ΔS_2^{PP} of the ERE from the free part as follows:

$$\Delta S_2^{\text{PP}}(x, \lambda) \equiv S_2^{\text{PP}}(V, \lambda) - S_2^{\text{PP}}(V, 0). \quad (3.22)$$

Notice that ΔS_2^{PP} only depends on the cross-ratio x and the Thirring coupling λ . Then, we can easily check that ΔS_2^{PP} is invariant under the modular S transformation: $x \mapsto 1 - x$;

$$\Delta S_2^{\text{PP}}(x, \lambda) = \Delta S_2^{\text{PP}}(1 - x, \lambda), \quad (3.23)$$

which ensures that ΔS_2^{PP} takes the local maximum or minimum at $x = 1/2$. Furthermore, the deviation ΔS_2^{PP} is invariant under the T-duality transformation (2.32):

$$\Delta S_2^{\text{PP}}(x, \lambda) = \Delta S_2^{\text{PP}}(x, \lambda_{\text{dual}}). \quad (3.24)$$

Also, ΔS_2^{PP} reduces to a simpler form in special cases as shown below:

- $\lambda = 1$: In this case, we can explicitly write down $\Delta S_2^{\text{PP}}(x, \lambda)$ in term of x ;

$$\Delta S_2^{\text{PP}}(x, \lambda = 1) = \log 2 - \log \left[1 + (1-x)^{\frac{1}{4}} + x^{\frac{1}{4}} - (x(1-x))^{\frac{1}{4}} \right]. \quad (3.25)$$

- $\lambda \rightarrow -1 + \delta$: At this point, the system becomes unstable and $\Delta S_2^{\text{PP}}(x, \lambda)$ shows a logarithmic divergence;

$$\lim_{\delta \rightarrow 0^+} \Delta S_2^{\text{PP}}(x, -1 + \delta) = \lim_{\delta \rightarrow 0^+} \frac{1}{2} \log \delta = -\infty. \quad (3.26)$$

- $x \rightarrow 0$: When the cross-ratio x is close to zero (or, equivalently one), the ERE $S_2^{\text{PP}}(V, \lambda)$ approaches the free one $S_2^{\text{PP}}(V, 0)$ for any λ ;

$$\lim_{x \rightarrow 0} \Delta S_2^{\text{PP}}(x, \lambda) = 0. \quad (3.27)$$

- $|\lambda| \ll 1$: When the coupling λ is quite small, we can expand the analytic formula (3.20) in powers of λ . After some manipulations, we arrive at the following result;

$$\begin{aligned} & \Delta S_2^{\text{PP}}(x, \lambda) \\ &= \lambda^2 \frac{\ell^2}{2\vartheta_3^4(i\ell)} \sum_{j=2}^4 \vartheta_j^2(i\ell) \left[(\partial_\ell \vartheta_j(i\ell))^2 - \vartheta_j(i\ell) \partial_\ell^2 \vartheta_j(i\ell) - \frac{\vartheta_j(i\ell) \partial_\ell \vartheta_j(i\ell)}{\ell} \right] + \mathcal{O}(\lambda^3). \end{aligned} \quad (3.28)$$

We should remark that the leading term starts at the second order of λ . This can be understood as follows. In the small coupling region, the duality relation (2.32) is approximated by $\lambda_{\text{dual}} \simeq -\lambda$, and the duality invariance (3.24) implies

$$\Delta S_2^{\text{PP}}(x, \lambda) = \Delta S_2^{\text{PP}}(x, -\lambda), \quad |\lambda| \ll 1, \quad (3.29)$$

which excludes a linear term in λ in the expansion.

Finally, we mention the MRI with $(n, N) = (2, 2)$ defined by

$$I_2^{\text{PP}}(V_1, V_2, \lambda) \equiv S_2^{\text{PP}}(V_1) + S_2^{\text{PP}}(V_2) - S_2^{\text{PP}}(V_1 \cup V_2), \quad (3.30)$$

where V_1 and V_2 are disjoint unions of the entangling region V : $V_1 = [u_1, v_1]$ and $V_2 = [u_2, v_2]$. The first and second terms are nothing but the EREs with $(n, N) = (2, 1)$ given by (3.13). The third term is the ERE with $(n, N) = (2, 2)$, and the analytic result has already been obtained in (3.20) by the boson-fermion duality. Therefore, by substituting (3.13) and (3.20) into (3.30), we get the MRI with $(n, N) = (2, 2)$ in the massless Thirring model;

$$I_2^{\text{PP}}(V_1, V_2, \lambda) = I_2^{\text{PP}}(V_1, V_2, 0) + \frac{1}{2} \log \left[\frac{1}{2\vartheta_3^4(i\ell)} \sum_{j=2}^4 \Xi_j(\lambda, i\ell) \right], \quad (3.31)$$

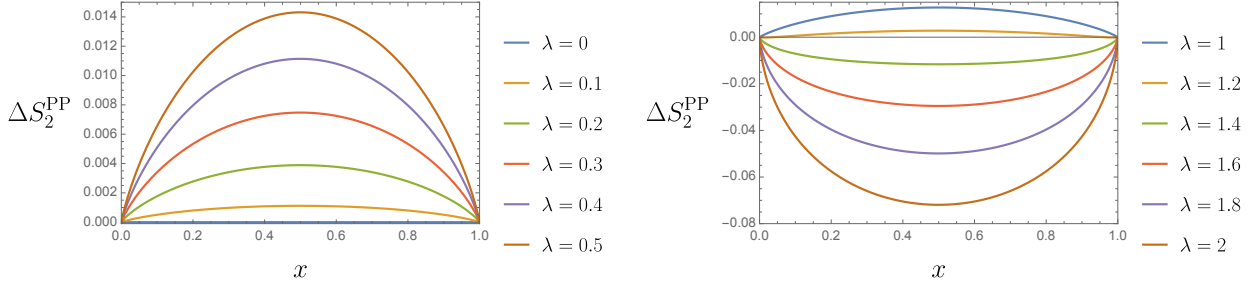


Figure 5. Cross-ratio dependence of the deviation ΔS_2^{PP} for $\lambda = 0, 0.1, 0.2, 0.3, 0.4, 0.5$ (left) and $\lambda = 1, 1.2, 1.4, 1.6, 1.8, 2$ (right).

where $I_2^{\text{PP}}(V_1, V_2, 0)$ is the contribution from the free theory:

$$I_2^{\text{PP}}(V_1, V_2, 0) = -\frac{1}{4} \log(1-x) . \quad (3.32)$$

In particular, when the cross-ratio x is very small and the Thirring coupling λ is in the range $1 - \sqrt{3} < \lambda < 1 + \sqrt{3}$, the MRI (3.31) can be approximated as follows;

$$I_2^{\text{PP}}(x, \lambda) \sim 4 \left(\frac{x}{16} \right)^{\frac{1}{2} \left(1 + \lambda + \frac{1}{1+\lambda} \right)} , \quad (3.33)$$

and clearly takes the positive value.⁴ We emphasize that the above result (3.33) is perfectly consistent with the universal asymptotic behavior of the MRI [18, equation (4.26)].

3.3 Parameter dependence of ERE and MRI

In section 3.2, we obtained the exact results of the ERE and MRI with $(n, N) = (2, 2)$ in the massless Thirring model. To grasp the physical meanings of these results, we explore the dependence of the ERE and MRI on the cross-ratio in section 3.3.1 and the Thirring coupling in section 3.3.2.

3.3.1 Cross-ratio dependence

We begin with examining the cross-ratio dependence of the ERE in (3.20) and the MRI in (3.31). In figure 5, we plot the deviation ΔS_2^{PP} by varying the cross-ratio x while fixing the Thirring coupling λ . Notice that both the left and right panels in figure 5 are symmetric under the map $x \mapsto 1-x$. Also, ΔS_2^{PP} takes the maximum or minimum value at $x = 1/2$. These behaviors are in accordance with the modular S symmetry (3.23). Furthermore, we can readily check that ΔS_2^{PP} becomes zero at $x = 0$ (or, equivalently $x = 1$) for any values of λ .

⁴This positivity is quite non-trivial since the MRI does not need to be positive unlike a mutual information.

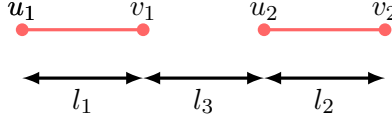


Figure 6. The definitions of the lengths ℓ_1 , ℓ_2 and ℓ_3 . The red lines are the entangling regions whose end points are denoted by u_1 , v_1 , u_2 and v_2 .

To elucidate the physical meaning of this phenomenon, we rewrite the cross-ratio x defined by (3.15) as follows;

$$x = \frac{\ell_1 \ell_2}{(\ell_1 + \ell_3)(\ell_2 + \ell_3)}, \quad (3.34)$$

where ℓ_1 , ℓ_2 and ℓ_3 are the lengths of the interval defined by (see also figure 6)

$$\ell_1 \equiv v_1 - u_1 \quad , \quad \ell_2 \equiv v_2 - u_2 \quad , \quad \ell_3 \equiv u_2 - v_1 . \quad (3.35)$$

From this expression, we can easily see that the limit $x \rightarrow 0$ is equivalent to the following limits of the interval lengths;

$$x \rightarrow 0 \quad \iff \quad \frac{\ell_1}{\ell_3} \rightarrow 0 \quad \text{or} \quad \frac{\ell_2}{\ell_3} \rightarrow 0 . \quad (3.36)$$

In the following, we concentrate on the two kinds of limits: $\ell_1 \rightarrow 0$ and $\ell_3 \rightarrow \infty$.

- $\ell_1 \rightarrow 0$:

In the limit $\ell_1 \rightarrow 0$, the entangling region V becomes the single interval $[u_2, v_2]$, and the ERE with $(n, N) = (2, 2)$ in the massless Thirring model becomes the ERE with $(n, N) = (2, 1)$ in the free theory,⁵

$$S_2^{\text{PP}}(V, \lambda) \longrightarrow S_2^{c=1}([u_2, v_2]) = \frac{1}{4} \log \left(\frac{\ell_2}{\epsilon} \right) , \quad (3.37)$$

hence the deviation ΔS_2^{PP} must vanish under the limit $\ell_1 \rightarrow 0$ by definition.

- $\ell_3 \rightarrow \infty$:

In the limit $\ell_3 \rightarrow \infty$, the two intervals are decoupled to each other, and the correlation between these intervals tends to vanish. Therefore, the ERE with $(n, N) = (2, 2)$ is reduced to the sum of the EREs with $(n, N) = (2, 1)$ in the free theory as follows;

$$S_2^{\text{PP}}(V, \lambda) \longrightarrow S_2^{c=1}([u_1, v_1]) + S_2^{c=1}([u_2, v_2]) . \quad (3.38)$$

That explains why ΔS_2^{PP} goes to zero in the limit $\ell_3 \rightarrow \infty$.

⁵Recall that the Thirring interaction does not contribute to the central charge.

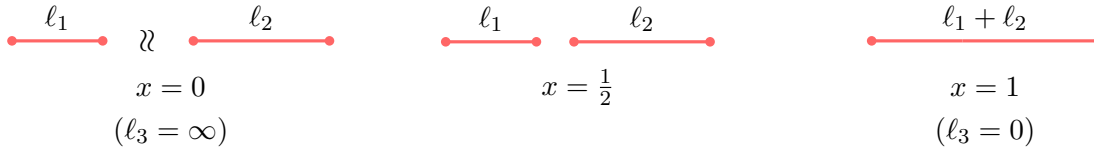


Figure 7. Locations of the two intervals in the case of $x = 0$ (left), $x = 1/2$ (middle) and $x = 1$ (right). In this figure, we fix the interval lengths ℓ_1 and ℓ_2 , hence the limits $x \rightarrow 0$ and $x \rightarrow 1$ are equivalent to the ones $\ell_3 \rightarrow \infty$ and $\ell_3 \rightarrow 0$, respectively. When $x = 0$, the two intervals are decoupled with each other, and the ERE can be written as the sum of the ones on the single interval (3.38). The contribution of the Thirring interaction to the ERE is locally maximized (or minimized) at $x = 1/2$. When $x = 1$, the two intervals are merged into the single interval with the length $\ell_1 + \ell_2$, and the ERE is given by (3.40).

Here, it is instructive to compare the ERE in the limit $x \rightarrow 1$ with (3.38). In a similar manner to $x \rightarrow 0$, the limit $x \rightarrow 1$ can be rephrased as

$$x \rightarrow 1 \quad \iff \quad \frac{\ell_3}{\ell_1} \rightarrow 0 \quad \text{and} \quad \frac{\ell_3}{\ell_2} \rightarrow 0. \quad (3.39)$$

We should notice that we can realize the limit $x \rightarrow 1$ by putting the two intervals together: $\ell_3 \rightarrow 0$ with the interval lengths ℓ_1 and ℓ_2 fixed. In this case, the ERE with $(n, N) = (2, 2)$ in the massless Thirring model reduces to the ERE with $(n, N) = (2, 1)$ of the interval length $\ell_1 + \ell_2$;

$$S_2^{\text{PP}}(V, \lambda) \longrightarrow S_2^{c=1}([u_1, v_2]) = \frac{1}{4} \log \left(\frac{\ell_1 + \ell_2}{\epsilon} \right). \quad (3.40)$$

Figure 7 illustrates the behaviors of the ERE in varying the cross-ratio x (or the distance ℓ_3 between two intervals) while keeping the interval lengths ℓ_1 and ℓ_2 .

Finally, we plot the MRI with $(n, N) = (2, 2)$ in (3.31) by changing the cross-ratio x in figure 8. In particular, from (3.38) and (3.40), the MRI with $(n, N) = (2, 2)$ behaves under the limits $\ell_3 \rightarrow \infty$ and $\ell_3 \rightarrow 0$ as follows;

$$\begin{aligned} I_2^{\text{PP}}(V_1, V_2, \lambda) &\longrightarrow 0, & \text{as } \ell_3 \rightarrow \infty, \\ I_2^{\text{PP}}(V_1, V_2, \lambda) &\longrightarrow \frac{1}{4} \log \left[\frac{\ell_1 \ell_2}{\epsilon(\ell_1 + \ell_2)} \right] = \infty, & \text{as } \ell_3 \rightarrow 0, \end{aligned} \quad (3.41)$$

which are completely consistent with the plot in figure 8.

3.3.2 Coupling dependence

We move on to study the Thirring coupling dependence of the ERE in (3.20) and the MRI in (3.31) with keeping the cross-ratio $x = 1/2$. In figure 9, we plot $\Delta S_2^{\text{PP}}(x = 1/2, \lambda)$ by changing λ . Notice that the positive coupling $\lambda \geq 0$ can be identified with the negative one $\lambda_{\text{dual}} = -\lambda/(1 + \lambda) \leq 0$ via the T-duality (2.32). Therefore, it is sufficient to consider only

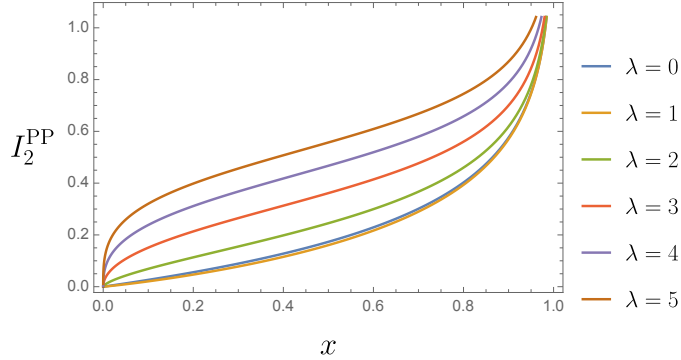


Figure 8. Cross-ratio dependence of the MRI for $\lambda = 0, 1, 2, 3, 4, 5$.

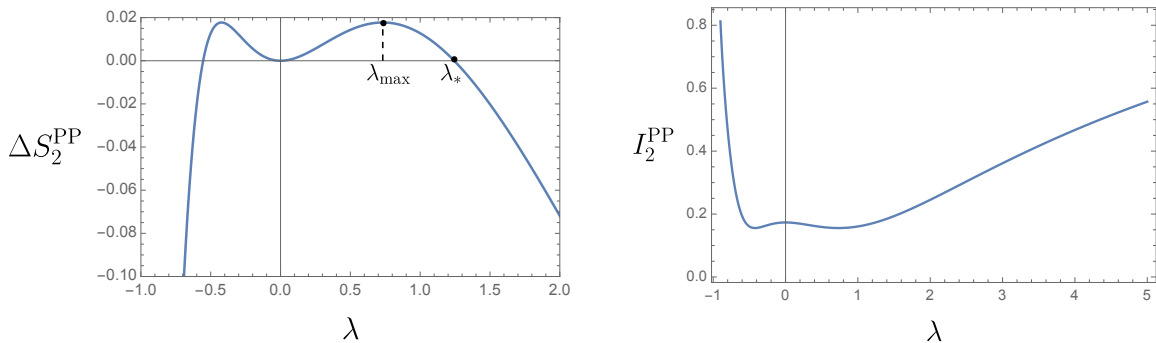


Figure 9. Thirring coupling dependence of the deviation $\Delta S_2^{\text{PP}}(x = 1/2, \lambda)$ is shown in the left panel and the MRI $I_2^{\text{PP}}(x = 1/2, \lambda)$ in the right panel.

the positive coupling region $\lambda \geq 0$. Let $\lambda_{\text{max}} > 0$ be the Thirring coupling that maximizes $\Delta S_2^{\text{PP}}(x = 1/2, \lambda)$. Then, we observe that $\Delta S_2^{\text{PP}}(x = 1/2, \lambda)$ monotonically increases in the range $0 \leq \lambda \leq \lambda_{\text{max}}$, and decreased in $\lambda \geq \lambda_{\text{max}}$. Also, we find out that there is a special point $\lambda_* \cong 1.244$ where $\Delta S_2^{\text{PP}}(x = 1/2, \lambda) = 0$, namely the ERE in the massless Thirring model is equal to the one in the free theory. Such a special point λ_* also appear for another value of cross-ratio x . Finally, we also plot the Thirring coupling dependence of the MRI in figure 9. The MRI in the massless Thirring model is always positive for any value of λ and shows a logarithmic divergence at $\lambda = \infty$.

3.4 EREs for other spin structures

We have been only concerned with the spin structure $\rho = \text{PP}$ and proceeded with the analysis on the ERE and MRI in the massless Thirring model. Here, we discuss the analytic properties of the ERE for the other spin structures, particularly focusing on $\rho = \text{AP}, \text{PA}$. In a similar manner to the spin structure $\rho = \text{PP}$, we can obtain exact results on the the EREs S_2^{AP} and

S_2^{PA} . First, by using the formula (3.19), we can express the EREs with $(n, N) = (2, 2)$ in terms of the torus partition functions:

$$\begin{aligned} S_2^{\text{AP}}(V, \lambda) &= \frac{1}{4} \log \left(\frac{v_1 - u_1}{\epsilon} \cdot \frac{v_2 - u_2}{\epsilon} \right) + \frac{1}{12} \log (2^8 x^{-2} (1 - x)) - \log Z_{\text{F}}(\text{PA}, \lambda, i\ell) , \\ S_2^{\text{PA}}(V, \lambda) &= \frac{1}{4} \log \left(\frac{v_1 - u_1}{\epsilon} \cdot \frac{v_2 - u_2}{\epsilon} \right) + \frac{1}{12} \log (2^8 x^{-2} (1 - x)) - \log Z_{\text{F}}(\text{AP}, \lambda, i\ell) . \end{aligned} \quad (3.42)$$

Furthermore, the fermionization dictionaries (2.27) and (2.26) map the torus partition functions of the massless Thirring model to those of the compact boson theory, hence we arrive at⁶

$$S_2^{\text{AP}}(V, \lambda) = S_2^{\text{AP}}(V, 0) - \frac{1}{2} \log \left[\frac{1}{2\vartheta_4^4(i\ell)} \sum_{j=2}^4 (1 - 2\delta_{2,j}) \Xi_j(\lambda, i\ell) \right] , \quad (3.43)$$

$$S_2^{\text{PA}}(V, \lambda) = S_2^{\text{PA}}(V, 0) - \frac{1}{2} \log \left[\frac{1}{2\vartheta_2^4(i\ell)} \sum_{j=2}^4 (1 - 2\delta_{4,j}) \Xi_j(\lambda, i\ell) \right] , \quad (3.44)$$

where $S_2^{\text{AP}}(V, 0)$ and $S_2^{\text{PA}}(V, 0)$ are the contributions from the free theories,

$$S_2^{\text{AP}}(V, 0) = \frac{1}{4} \log \left(\frac{v_1 - u_1}{\epsilon} \cdot \frac{v_2 - u_2}{\epsilon} \right) - \frac{1}{4} \log(1 - x) . \quad (3.45)$$

$$S_2^{\text{PA}}(V, 0) = \frac{1}{4} \log \left(\frac{v_1 - u_1}{\epsilon} \cdot \frac{v_2 - u_2}{\epsilon} \right) + \frac{1}{4} \log(x^{-2}(1 - x)) . \quad (3.46)$$

As in the case of $\rho = \text{PP}$, it is convenient to define the deviations ΔS_2^{AP} and ΔS_2^{PA} as follows:

$$\Delta S_2^{\text{AP}}(V, \lambda) \equiv S_2^{\text{AP}}(V, \lambda) - S_2^{\text{AP}}(V, 0) , \quad \Delta S_2^{\text{PA}}(V, \lambda) \equiv S_2^{\text{PA}}(V, \lambda) - S_2^{\text{PA}}(V, 0) . \quad (3.47)$$

The dependence on the cross-ratio and the Thirring coupling are shown in figure 10 and figure 11, respectively. In particular, as suggested by figure 10, ΔS_2^{AP} and ΔS_2^{PA} satisfy the following relation:

$$\Delta S_2^{\text{AP}}(x, \lambda) = \Delta S_2^{\text{PA}}(1 - x, \lambda) . \quad (3.48)$$

We can easily prove this formula by noticing that the modular S transformation exchanges the spin structure AP with PA and the cross-ratio x with $1 - x$.

Finally, we remark that the EREs S_2^{AP} and S_2^{PA} reduce to the ERE S_2^{PP} in the limits $x \rightarrow 0$ and $x \rightarrow 1$, respectively;

$$S_2^{\text{AP}}(x, \lambda) \longrightarrow S_2^{\text{PP}}(x, \lambda) , \quad \text{as } x \rightarrow 0 , \quad (3.49)$$

$$S_2^{\text{PA}}(x, \lambda) \longrightarrow S_2^{\text{PP}}(x, \lambda) , \quad \text{as } x \rightarrow 1 . \quad (3.50)$$

⁶We can also derive the ERE with the spin structure $\rho = \text{AA}$ only for the negative coupling $\lambda < 0$;

$$S_2^{\text{AA}}(V, \lambda < 0) = \frac{1}{4} \log \left(\frac{v_1 - u_1}{\epsilon} \cdot \frac{v_2 - u_2}{\epsilon} \right) + \frac{1}{12} \log (2^{14} x^{-2} (1 - x)) - \frac{1}{2} \log \left[\frac{1}{\eta^2(i\ell)} \sum_{j=2}^4 (2\delta_{3,j} - 1) \Xi_j(\lambda, i\ell) \right] .$$

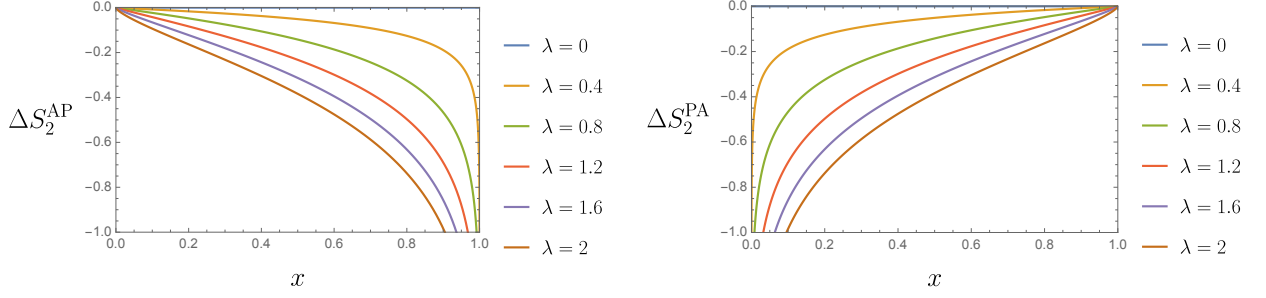


Figure 10. Cross-ratio dependence of the deviations ΔS_2^{AP} (left) and ΔS_2^{PA} (right) for $\lambda = 0, 0.4, 0.8, 1.2, 1.6, 2$.

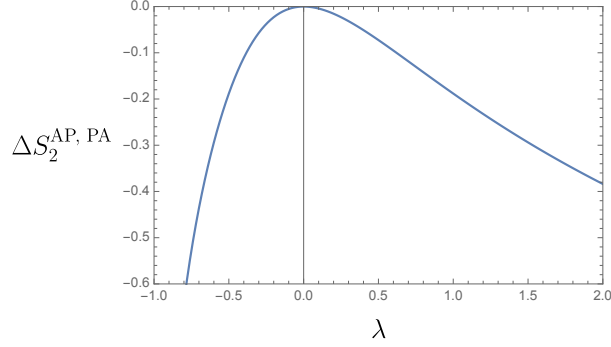


Figure 11. Thirring coupling dependence of the deviation $\Delta S_2^{\text{AP}}(x = 1/2, \lambda) = \Delta S_2^{\text{PA}}(x = 1/2, \lambda)$.

We can derive these asymptotic behaviors by using the results (3.43) and (3.44), but it is more instructive to understand them from the view point of the topological defect. Since the fermionic theory has the global symmetry $\mathbb{Z}_2^{\text{F}} : \psi \mapsto -\psi$, we can obtain the EREs S_2^{AP} and S_2^{PA} by inserting the \mathbb{Z}_2^{F} topological line into one-cycles on the two-sheeted manifold $\Sigma_{2,2}$ ⁷ as depicted in figure 12. Under this setup, we first take the limit $x \rightarrow 0$ of the ERE S_2^{AP} . We must recall that, as discussed in section 3.3.1, the limit $x \rightarrow 0$ can be realized by vanishing the interval $[u_1, v_1]$. As a result, the \mathbb{Z}_2^{F} topological line becomes contractible, namely trivial, and then the ERE S_2^{AP} reduces to S_2^{PP} (see figure 13). Similarly, if we take the limit $x \rightarrow 1$ in the ERE S_2^{PA} , the two intervals merge and the \mathbb{Z}_2^{F} topological line becomes trivial. This observation is illustrated in figure 14 and naturally explains the asymptotic behavior of the ERE S_2^{PA} in (3.50).

⁷We assume that the original two-sheeted manifold $\Sigma_{2,2}$ is equipped with the periodic spin structure $\rho = \text{PP}$.

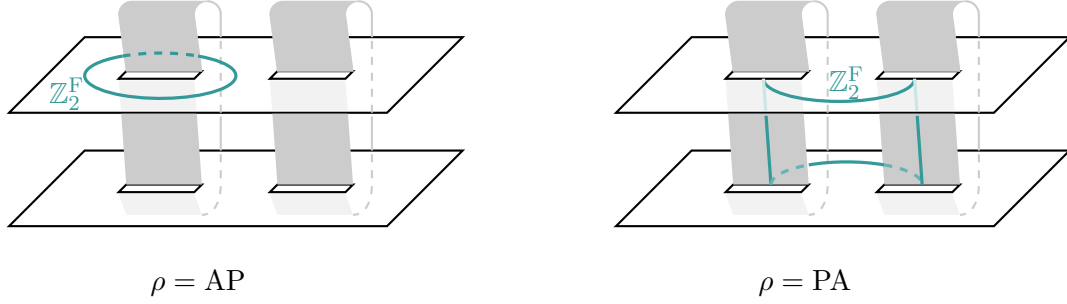


Figure 12. Fermionic theories with the spin structures $\rho = \text{AP}$ (left), PA (right) on the two-sheeted manifold $\Sigma_{2,2}$ can be obtained by wrapping the \mathbb{Z}_2^{F} topological line (green line) in one cycle on $\Sigma_{2,2}$.

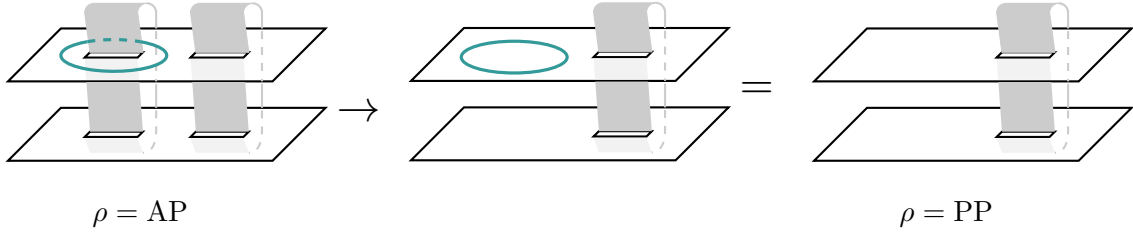


Figure 13. Pictorial explanation on the asymptotic behavior (3.49) of the ERE S_2^{AP} . The green line means the \mathbb{Z}_2^{F} defect line. By taking the limit $x \rightarrow 0$, the interval $[u_1, v_1]$ vanishes, and the \mathbb{Z}_2^{F} topological line becomes trivial. Then, the ERE S_2^{AP} is reduced to the one with the spin structure $\rho = \text{PP}$.

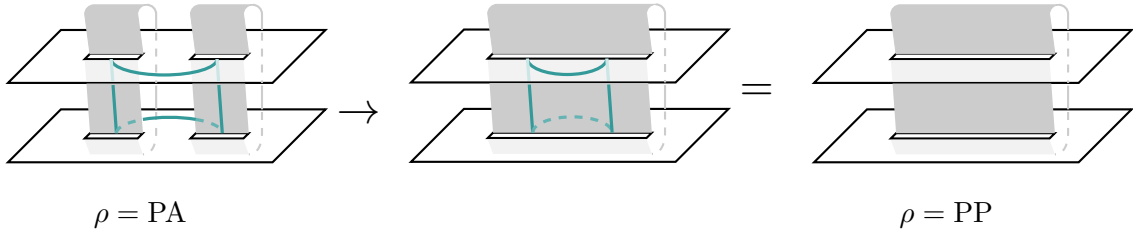


Figure 14. Pictorial explanation on the asymptotic behavior (3.50) of the ERE S_2^{PA} . By taking the limit $x \rightarrow 1$, two intervals get merged into the single one, and the \mathbb{Z}_2^{F} topological line becomes trivial. Then, the ERE S_2^{PA} is reduced to the one S_2^{PP} .

4 Conclusion and Discussion

In this paper, we derived exact results on the ERE and MRI with $(n, N) = (2, 2)$ in the massless Thirring model by combining the replica method with the boson-fermion duality. We first rewrote the ERE with $(n, N) = (2, 2)$ in terms of the torus partition function of the massless Thirring model via the conformal map. Then, we exploited the boson-fermion duality between the massless Thirring model and a free compact boson theory, and expressed the torus partition function of the former in terms of those of the latter. We also explored the physical properties of the ERE and MRI with $(n, N) = (2, 2)$ in the massless Thirring model by examining the dependence on the cross-ratio and Thirring coupling for various spin structures.

While we only dealt with the massless Thirring model, this serves as the first step toward applying the boson-fermion duality to examine the ERE and MRI. We believe that the boson-fermion duality will become a fundamental tool for comprehending quantum information quantities and will contribute to a deeper understanding of the dynamics of QFTs.

This work opens several interesting directions for further studies, some of which include the followings.

First, we can generalize our analysis to include multiple replica sheets or intervals. As mentioned in Introduction, the n -sheeted manifold $\Sigma_{n,N}$ transforms into a Riemann surface of genus $g = (n-1)(N-1)$ through a conformal map, and the boson-fermion duality also applies to such cases [27]. Since the partition function of a free compact boson on a higher genus Riemann surface has been previously studied in [24, 25, 32], it is possible to extend our work to higher genus cases given a conformal map from a singular Riemann surface $\Sigma_{n,N}$ to a smooth one as in [31] for the $n = N = 2$ case.

Secondly, our work may be extended to the Thirring model with a mass term. Under boson-fermion duality, the fermion mass term is known to be mapped to the sine-Gordon potential [29]. When the mass term is small, we can take into account the mass-correction to an ERE and an MRI as a relevant perturbation of CFT. (For the free massive fermion theory, a perturbative calculation has been performed in [14, 33].) It is intriguing to apply the conformal perturbation theory to the massive Thirring model and derive the corrections to the ERE and MRI obtained in this paper.

Finally, in the moduli space of $c = 1$ bosonic theory, there are some special points where supersymmetries become enhanced. On the one hand, the n -th supersymmetric Rényi entropy [20] of arbitrary intervals in the $\mathcal{N} = (2, 2)$ superconformal field theory has been derived in [34, 35]. It may be interesting to compare the result obtained in this paper with the supersymmetric Rényi entropy.

Acknowledgments

The work of T.N. was supported in part by the JSPS Grant-in-Aid for Scientific Research (C) No.19K03863, Grant-in-Aid for Scientific Research (A) No. 21H04469, and Grant-in-Aid for Transformative Research Areas (A) “Extreme Universe” No. 21H05182 and No. 21H05190. The work of S.S. was supported by Grant-in-Aid for JSPS Fellows No. 23KJ1533.

A Formulas on theta function and Dedekind eta function

In this appendix, we list some formulas relating the theta function and the Dedekind eta function which are widely used throughout this paper.

Jacobi identity.

$$\vartheta_3(\tau)^4 - \vartheta_2(\tau)^4 - \vartheta_4(\tau)^4 = 0 . \quad (\text{A.1})$$

Eta and theta relation.

$$2\eta(\tau)^3 = \vartheta_2(\tau)\vartheta_3(\tau)\vartheta_4(\tau) . \quad (\text{A.2})$$

Doubling identities.

$$\vartheta_2(2\tau) = \left(\frac{\vartheta_3(\tau)^2 - \vartheta_4(\tau)^2}{2} \right)^{\frac{1}{2}} , \quad (\text{A.3})$$

$$\vartheta_3(2\tau) = \left(\frac{\vartheta_3(\tau)^2 + \vartheta_4(\tau)^2}{2} \right)^{\frac{1}{2}} , \quad (\text{A.4})$$

$$\vartheta_4(2\tau) = (\vartheta_3(\tau) \vartheta_4(\tau))^{\frac{1}{2}} . \quad (\text{A.5})$$

Modular properties.

$$\vartheta_2\left(-\frac{1}{\tau}\right) = \sqrt{-i\tau} \vartheta_4(\tau) , \quad (\text{A.6})$$

$$\vartheta_3\left(-\frac{1}{\tau}\right) = \sqrt{-i\tau} \vartheta_3(\tau) , \quad (\text{A.7})$$

$$\vartheta_4\left(-\frac{1}{\tau}\right) = \sqrt{-i\tau} \vartheta_2(\tau) , \quad (\text{A.8})$$

$$\eta\left(-\frac{1}{\tau}\right) = \sqrt{-i\tau} \eta(\tau) . \quad (\text{A.9})$$

Asymptotic behaviors.

$$\begin{aligned}\vartheta_2(i\ell) &\sim 2e^{-\frac{\pi\ell}{4}} , \\ \vartheta_3(i\ell) &\sim 1 + 2e^{-\pi\ell} , \quad \text{as } \ell \sim \infty , \\ \vartheta_4(i\ell) &\sim 1 - 2e^{-\pi\ell} .\end{aligned}\tag{A.10}$$

$$\begin{aligned}\vartheta_2(i\ell) &\sim \ell^{-1/2} , \\ \vartheta_3(i\ell) &\sim \ell^{-1/2} , \quad \text{as } \ell \sim 0 , \\ \vartheta_4(i\ell) &\sim 2\ell^{-1/2} e^{-\frac{\pi}{4\ell}} .\end{aligned}\tag{A.11}$$

B Detailed calculations of (2.25)

Here, we derive (2.25) by evaluating the summation in the fermionization dictionary (2.24). For the sake of simplicity, we will employ the following shorthand notations;

$$\vartheta_j \equiv \vartheta_j^2(i\ell(1+\lambda)) \quad , \quad \tilde{\vartheta}_j \equiv \vartheta_j^2\left(\frac{i\ell}{1+\lambda}\right) \quad , \quad j = 1, 2, 3 .\tag{B.1}$$

In the case of $\tilde{\rho} = AA$, the dictionary (2.13) reads

$$Z_F[AA, \lambda, i\ell] = \frac{1}{2} (Z_B[00, \lambda, i\ell] + Z_B[01, \lambda, i\ell] + Z_B[10, \lambda, i\ell] - Z_B[11, \lambda, i\ell]) .\tag{B.2}$$

We first calculate the first two summation $Z_B[00, \lambda, i\ell] + Z_B[01, \lambda, i\ell]$. By substituting (2.18) and (2.19) into this, we can massage in the following way;

$$\begin{aligned}Z_B[00, \lambda, i\ell] + Z_B[01, \lambda, i\ell] &= \frac{1}{\sqrt{2}\eta(i\ell)^2} (\vartheta_3^2 + \vartheta_2^2)^{1/2} \left[\left(\tilde{\vartheta}_3^2 + \tilde{\vartheta}_4^2 \right)^{1/2} + \left(\tilde{\vartheta}_3^2 - \tilde{\vartheta}_4^2 \right)^{1/2} \right] \\ &= \frac{1}{\eta(i\ell)^2} [\vartheta_3^2 + \vartheta_2^2]^{1/2} \left[\tilde{\vartheta}_3^2 + \left(\tilde{\vartheta}_3^4 - \tilde{\vartheta}_4^4 \right)^{1/2} \right]^{1/2} \\ &= \frac{1}{\eta(i\ell)^2} \left[(\vartheta_3^2 + \vartheta_2^2) \left(\tilde{\vartheta}_3^2 + \tilde{\vartheta}_2^2 \right) \right]^{1/2} ,\end{aligned}\tag{B.3}$$

where in the final line, we used the Jacobi identity (A.1). In a very similar manner to the above, we can evaluate the rest summation in (B.2) and the result is

$$Z_B[10, \lambda, i\ell] - Z_B[11, \lambda, i\ell] = \frac{1}{\eta(i\ell)^2} \left[(\vartheta_3^2 - \vartheta_2^2) \left(\tilde{\vartheta}_3^2 - \tilde{\vartheta}_2^2 \right) \right]^{1/2} .\tag{B.4}$$

By putting together (B.3) and (B.4) into (B.2), we can derive (2.25) as follows;

$$\begin{aligned}Z_F[AA, \lambda, i\ell] &= \frac{1}{2\eta(i\ell)^2} \left[\left[(\vartheta_3^2 + \vartheta_2^2) \left(\tilde{\vartheta}_3^2 + \tilde{\vartheta}_2^2 \right) \right]^{1/2} + \left[(\vartheta_3^2 - \vartheta_2^2) \left(\tilde{\vartheta}_3^2 - \tilde{\vartheta}_2^2 \right) \right]^{1/2} \right] \\ &= \frac{1}{\sqrt{2}\eta(i\ell)^2} \left[\vartheta_2^2 \tilde{\vartheta}_2^2 + \vartheta_3^2 \tilde{\vartheta}_3^2 + \left[(\vartheta_3^4 - \vartheta_2^4) \left(\tilde{\vartheta}_3^4 - \tilde{\vartheta}_2^4 \right) \right]^{1/2} \right]^{1/2} \\ &= \frac{1}{\sqrt{2}\eta(i\ell)^2} \left[\vartheta_2^2 \tilde{\vartheta}_2^2 + \vartheta_3^2 \tilde{\vartheta}_3^2 + \vartheta_4^2 \tilde{\vartheta}_4^2 \right] \\ &= (2.25) ,\end{aligned}\tag{B.5}$$

where we again used the Jacobi identity (A.1) in the third line. By taking similar steps above, we can get other formulas (2.26)-(2.28).

References

- [1] A. Kitaev and J. Preskill, *Topological entanglement entropy*, *Phys. Rev. Lett.* **96** (2006) 110404 [[hep-th/0510092](#)].
- [2] M. Levin and X.-G. Wen, *Detecting Topological Order in a Ground State Wave Function*, *Phys. Rev. Lett.* **96** (2006) 110405 [[cond-mat/0510613](#)].
- [3] C. Holzhey, F. Larsen and F. Wilczek, *Geometric and renormalized entropy in conformal field theory*, *Nucl. Phys. B* **424** (1994) 443 [[hep-th/9403108](#)].
- [4] G. Vidal, J. I. Latorre, E. Rico and A. Kitaev, *Entanglement in quantum critical phenomena*, *Phys. Rev. Lett.* **90** (2003) 227902 [[quant-ph/0211074](#)].
- [5] P. Calabrese and J. L. Cardy, *Entanglement entropy and quantum field theory*, *J. Stat. Mech.* **0406** (2004) P06002 [[hep-th/0405152](#)].
- [6] A. R. Its, B.-Q. Jin and V. E. Korepin, *Entanglement in the xy spin chain*, *Journal of Physics A: Mathematical and General* **38** (2005) 2975.
- [7] S. Ryu and T. Takayanagi, *Holographic derivation of entanglement entropy from AdS/CFT*, *Phys. Rev. Lett.* **96** (2006) 181602 [[hep-th/0603001](#)].
- [8] S. Ryu and T. Takayanagi, *Aspects of Holographic Entanglement Entropy*, *JHEP* **08** (2006) 045 [[hep-th/0605073](#)].
- [9] P. Calabrese and J. Cardy, *Entanglement entropy and conformal field theory*, *J. Phys. A* **42** (2009) 504005 [[0905.4013](#)].
- [10] H. Casini and M. Huerta, *Entanglement entropy in free quantum field theory*, *J. Phys. A* **42** (2009) 504007 [[0905.2562](#)].
- [11] T. Nishioka, S. Ryu and T. Takayanagi, *Holographic Entanglement Entropy: An Overview*, *J. Phys. A* **42** (2009) 504008 [[0905.0932](#)].
- [12] M. Rangamani and T. Takayanagi, *Holographic Entanglement Entropy*, vol. 931. Springer, 2017, [10.1007/978-3-319-52573-0](#), [[1609.01287](#)].
- [13] T. Nishioka, *Entanglement entropy: holography and renormalization group*, *Rev. Mod. Phys.* **90** (2018) 035007 [[1801.10352](#)].
- [14] H. Casini, C. D. Fosco and M. Huerta, *Entanglement and alpha entropies for a massive Dirac field in two dimensions*, *J. Stat. Mech.* **0507** (2005) P07007 [[cond-mat/0505563](#)].
- [15] I. R. Klebanov, S. S. Pufu, S. Sachdev and B. R. Safdi, *Rényi Entropies for Free Field Theories*, *JHEP* **04** (2012) 074 [[1111.6290](#)].
- [16] P. Calabrese, J. Cardy and E. Tonni, *Entanglement entropy of two disjoint intervals in conformal field theory*, *J. Stat. Mech.* **0911** (2009) P11001 [[0905.2069](#)].
- [17] P. Calabrese, J. Cardy and E. Tonni, *Entanglement entropy of two disjoint intervals in conformal field theory II*, *J. Stat. Mech.* **1101** (2011) P01021 [[1011.5482](#)].

- [18] M. Headrick, *Entanglement Rényi entropies in holographic theories*, *Phys. Rev. D* **82** (2010) 126010 [[1006.0047](#)].
- [19] M. A. Metlitski, C. A. Fuertes and S. Sachdev, *Entanglement Entropy in the $O(N)$ model*, *Phys. Rev. B* **80** (2009) 115122 [[0904.4477](#)].
- [20] T. Nishioka and I. Yaakov, *Supersymmetric Rényi Entropy*, *JHEP* **10** (2013) 155 [[1306.2958](#)].
- [21] W. E. Thirring, *A Soluble relativistic field theory?*, *Annals Phys.* **3** (1958) 91.
- [22] M. Headrick, A. Lawrence and M. Roberts, *Bose-Fermi duality and entanglement entropies*, *J. Stat. Mech.* **1302** (2013) P02022 [[1209.2428](#)].
- [23] A. Kitaev, *Unpaired Majorana fermions in quantum wires*, *Phys. Usp.* **44** (2001) 131 [[cond-mat/0010440](#)].
- [24] L. Alvarez-Gaume, G. W. Moore and C. Vafa, *Theta Functions, Modular Invariance and Strings*, *Commun. Math. Phys.* **106** (1986) 1.
- [25] L. Alvarez-Gaume, J. B. Bost, G. W. Moore, P. C. Nelson and C. Vafa, *Bosonization on Higher Genus Riemann Surfaces*, *Commun. Math. Phys.* **112** (1987) 503.
- [26] P. H. Ginsparg, *APPLIED CONFORMAL FIELD THEORY*, in *Les Houches Summer School in Theoretical Physics: Fields, Strings, Critical Phenomena*, 9, 1988, [hep-th/9108028](#).
- [27] A. Karch, D. Tong and C. Turner, *A Web of 2d Dualities: \mathbf{Z}_2 Gauge Fields and Arf Invariants*, *SciPost Phys.* **7** (2019) 007 [[1902.05550](#)].
- [28] Y. Tachikawa, “Topological phases and relativistic QFTs.” <https://member.ipmu.jp/yuji.tachikawa/lectures/2018-cern-rikkyo/>.
- [29] S. R. Coleman, *The Quantum Sine-Gordon Equation as the Massive Thirring Model*, *Phys. Rev. D* **11** (1975) 2088.
- [30] P. Di Francesco, P. Mathieu and D. Senechal, *Conformal Field Theory*, Graduate Texts in Contemporary Physics. Springer-Verlag, New York, 1997, [10.1007/978-1-4612-2256-9](#).
- [31] O. Lunin and S. D. Mathur, *Correlation functions for M^N/S_N orbifolds*, *Commun. Math. Phys.* **219** (2001) 399 [[hep-th/0006196](#)].
- [32] R. Dijkgraaf, E. P. Verlinde and H. L. Verlinde, *$C = 1$ Conformal Field Theories on Riemann Surfaces*, *Commun. Math. Phys.* **115** (1988) 649.
- [33] C. P. Herzog and T. Nishioka, *Entanglement Entropy of a Massive Fermion on a Torus*, *JHEP* **03** (2013) 077 [[1301.0336](#)].
- [34] A. Giveon and D. Kutasov, *Supersymmetric Rényi entropy in CFT_2 and AdS_3* , *JHEP* **01** (2016) 042 [[1510.08872](#)].
- [35] H. Mori, *Supersymmetric Rényi entropy in two dimensions*, *JHEP* **03** (2016) 058 [[1512.02829](#)].